Electronic Spectral Studies of Molybdenyl Complexes: Implications for Oxomolybdenum Enzymes

Michael D. Carducci,[†] Carl Brown,[‡] Edward I. Solomon,*[,‡] and John H. Enemark*[,†]

Contribution from the Department of Chemistry, University of Arizona, Tucson, Arizona 85721, and the Department of Chemistry, Stanford University, Stanford, California 94305

Received June 20, 1994[⊗]

Abstract: Magnetic circular dichroism spectroscopy (MCD) has been used to assign the optical spectra in high- and low-symmetry molybdenyl complexes. High-resolution single crystal polarized absorption spectra of $[PPh_4][MoOCl_4]$ and $[AsPh_4][MoOCl_4(H_2O)]$ show two ligand field transitions whose polarization, MCD, and vibronic fine structure are compatible with the previously accepted assignments $^2E \leftarrow {}^2B_2$ (15000 and 13000 cm^{-1}, respectively) and $^2B_1 \leftarrow {}^2B_2$ (23000 cm^{-1} in both). In the case of $[AsPh_4][MoOCl_4(H_2O)]$, the splitting of the ^2E by spin-orbit coupling is clearly visible and a spin-orbit coupling constant of 810(2) cm^{-1} has been measured. At higher energies, four charge transfer transitions arising from nonbonding chloride orbitals to the metal d_{xy} orbital have been identified. The absorption and MCD spectra of $LMoOX_2$ complexes (where L is hydrotris(3,5-dimethyl-1-pyrazolyl)borate and X = O, Cl, or S) which possess only C_s symmetry can be interpreted within the same framework of ligand field and ligand π to metal charge transfer transitions adopted for $[AsPh_4][MoOCl_4(H_2O)]$. Although remarkably consistent in other respects, the MCD spectra of the lowest energy ligand field transition of the $LMoOX_2$ compounds show that the ordering of the d orbitals that are π antibonding with respect to the molybdenyl group depends upon the equatorial donor ligands. For $LMoO^{2+}$ complexes of $^-SCH_2CH_2S^-$ (saturated chelate skeleton) and toluene-3,4-dithiolate (aromatic chelate skeleton), the features between ~9000 and 16000 cm^{-1} are assigned to charge transfer transitions from filled sulfur out-of-plane π orbitals to d_{xy} that overlap with the lowest lying ligand field bands. The pattern of intense MCD peaks between 17000 and 35000 cm^{-1} (nearly identical in these compounds) is assigned to charge transfer transitions from filled out-of-plane sulfur π orbitals to the oxomolybdenum π-antibonding orbitals, $d_{xz,yz}$. On the basis of the results of these molybdenyl model complexes, an interpretation is proposed for the recently reported MCD spectra of DMSO reductase. The spectroscopic studies of $LMoO(SCH_2CH_2S)$ and LMoO(toluene-3,4-dithiolate) also provide insight into the general role of sulfur coordination in oxo-molybdenum enzymes. The filled sulfur π-donor orbitals are close in energy to the molybdenum d orbitals; π donation from these filled sulfur orbitals competes with π donation from the terminal oxo groups and weakens the Mo=O bond, thereby facilitating oxygen atom transfer chemistry. The filled sulfur π orbitals also provide an effective low energy super exchange pathway for the one-electron transfers from d_{xy} that interconvert the Mo(IV,V,VI) states during the catalytic cycle.

I. Introduction

The role of molybdenum in enzymes that catalyze net oxygen atom transfer reactions (e.g. xanthine oxidase, sulfite oxidase, nitrate reductase) continues to stimulate interest in oxomolybdenum chemistry.[1-6] No crystal structure is yet available for any of these pterin-containing molybdenum enzymes, but EXAFS studies[7,8] at the Mo K-edge and EPR studies[9-11] of the transient molybdenum(V) states that appear during enzyme turnover support an oxo-Mo active site with at least two sulfur donor atoms. *In vivo* degradation studies and the *nit-1* assay have lead to the proposal that all of these enzymes possess a common molybdenum cofactor (Figure 1a) in which the molybdenum atom is coordinated by two sulfur atoms of the dithiolene side chain of molybdopterin.[12] Electronic absorption spectroscopy has not been particularly useful for investigating

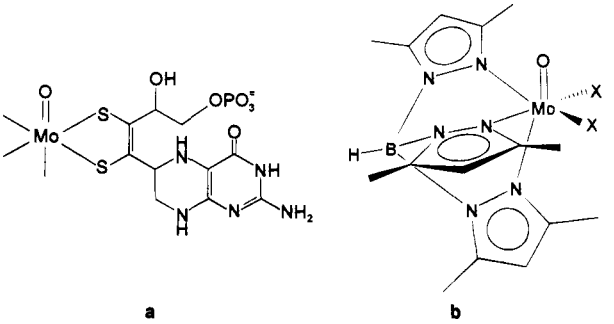

a b

Figure 1. (a) Proposed structure of the molybdenum cofactor,[12] drawn to emphasize the possible cis-dithiolene coordination of the molybdenyl group and (b) structure of the $LMoOX_2$ (where L is hydrotris(3,5-dimethyl-1-pyrazolyl)borate and X = O, Cl, or S) model compounds.

[†] University of Arizona.
[‡] Stanford University.
[⊗] Abstract published in *Advance ACS Abstracts*, November 15, 1994.

(1) Enemark, J. H.; Young, C. G. *Adv. Inorg. Chem.* **1993**, *40*, 1-88.
(2) Pilato, R. S.; Steifel, E. I. In *Bioinorganic Catalysis*; Reedijk, J., Ed.; Marcel Dekker, Inc.: New York, NY, 1993; pp 131-186.
(3) *Molybdenum and Molybdenum-containing Enzymes*; Coughlan, M., Ed.; Pergamon Press: New York, NY, 1980.
(4) *Molybdenum Enzymes*; Spiro, T., Ed.; John Wiley and Sons: New York, NY, 1985.
(5) Bray, R. C. *Q. Rev. Biophys.* **1988**, *21*, 299-329.
(6) Burgmayer, S. J. N.; Stiefel, E. I. *J. Chem. Educ.* **1985**, *62*, 943-953.
(7) Cramer, S. P.; Wahl, R.; Rajagopalan, K. V. *J. Am. Chem. Soc.* **1981**, *103*, 7721-7727.
(8) George, G. N.; Kipke, C. A.; Prince, R. C.; Sunde, R. A.; Enemark, J. H.; Cramer, S. P. *Biochemistry* **1989**, *28*, 5075.
(9) George, G. N.; Bray, R. C. *Biochemistry* **1988**, *27*, 3603.
(10) Bray, R. C. *Biol. Magn. Reson.* **1980**, *2*, 45.
(11) Dhawan, I. K.; Pacheco, A.; Enemark, J. H. *J. Am. Chem. Soc.* **1994**, *116*, 7911-7912.
(12) Rajagopalan, K. V. *Adv. Enzymol. Relat. Areas Mol. Biol.* **1991**, *64*, 215-290.

0002-7863/94/1516-11856$04.50/0

the molecular and electronic structure of the molybdenum center because most enzymes of this class contain additional prosthetic groups such as hemes, iron sulfur centers, and flavins whose intense electronic absorptions obscure any absorbance that might arise from the oxomolybdenum center of the pterin-containing molybdenum cofactor.[1] In direct contrast to this situation, the electronic spectroscopy of many simple complexes of the molybdenyl fragment ($[MoO]^{3+}$) and molecular orbital interpretations of the bonding in such complexes have been the subject of discussion for over 30 years. Starting with the initial investigations of Jørgenson[13] and the molecular orbital interpretations of Gray and co-workers,[14,15] a picture of the bonding in d^1 monooxo complexes has emerged which Collison[16] has shown consistently explains the ligand field transitions of V, Cr, and Mo.

Magnetic circular dichroism (MCD) spectroscopy is an extremely powerful technique for investigating the electronic structure of metal centers.[17-20] It compliments traditional absorption spectroscopy by probing the effects of Zeeman splittings on the ground and excited states. This additional information can provide definitive assignments and help deconvolute overlapping transitions since it may be positive or negative in sign. In addition, the inherent low-temperature enhancement of the intensity of the MCD of paramagnetic systems can make their study possible, even in the presence of other strongly absorbing diamagnetic chromophores. Variable-temperature MCD of enzymes poised in the Mo(V) state, and with other strongly absorbing prosthetic groups (hemes, iron sulfur centers, flavins) in *diamagnetic states*, offers the hope of directly probing the electronic structure of the molybdenum center in these complex multimetal center systems. Preliminary variable-temperature MCD spectra by Peterson *et al.*[21] on inhibited desulfo xanthine oxidase provided encouraging evidence that MCD could be used to study the molybdenum centers of enzymes despite the presence of other more strongly absorbing chromophores. While the work described herein was in progress, the enzyme DMSO reductase was discovered. This enzyme contains the molybdenum cofactor (as molybdopterin guanine dinucleotide[22]) as the only prosthetic group. Low-temperature MCD spectra of native DMSO reductase from *Rhodobacter capsulatus*[23] and of the glycerol-inhibited enzyme from *Rhodobacter sphaeroides*[24] show rich and distinctive MCD spectra between 300 and 800 nm that have been assigned to π-dithiolene to Mo(V) charge transfer transitions.

An important prerequisite to detailed understanding of the MCD spectra from molybdenum enzymes is a systematic investigation and analysis of the MCD spectra from well-characterized molybdenum(V) complexes. The object of this study has been to explore the application of MCD spectroscopy to such molybdenyl complexes. This study commences with a detailed reinvestigation of the polarized absorption spectra and complementary new single-crystal and orientationally averaged MCD spectra of the high-symmetry $[MoOCl_4]^-$ (C_{4v}) and $[MoOCl_4(H_2O)]^-$ ions. From there we proceed to lower symmetry model complexes of the type $LMoOX_2$ (where L is hydrotris(3,5-dimethyl-1-pyrazolyl)borate and X = Cl, O, or S donor atoms, Figure 1b). The bulky ligand, L, is an inexpensive, easily synthesized tridentate ligand that stabilizes a wide range of mononuclear oxo-Mo(V) complexes of the general form $LMoOX_2$, where X is a monoanionic ligand.[25] The steric requirements of L impose six-coordinate *fac* stereochemistry on the complexes and consequently the O and X ligands are mutually cis to one another. The $LMoOX_2$ complexes investigated here have effective C_s coordination symmetry. We conclude with a discussion of the implications of the MCD spectra of these structurally defined model complexes for the recently reported low-temperature MCD spectra for DMSO reductases[23,24] and a discussion of the insight that these electronic structural studies provide for the catalytic reactions of oxomolybdenum enzymes.

II. Experimental Methods

1. Preparation of Compounds and Structural Information. $[PPh_4][MoOCl_4]$. Dry, degassed CH_2Cl_2 (20 mL) was added to 0.30 g (1.1 mmol) of $MoCl_5$ and 0.41 g (1.1 mmol) of dried PPh_4Cl in a Schlenk flask under N_2. To the red/brown slurry was added H_2O or MeOH in small (0.1 mL, totaling ~0.5 mL) aliquots until a clear emerald green solution resulted. The solution was allowed to evaporate overnight under a very slow stream of N_2 gas, producing large optical quality tetragonally shaped crystals. X-ray crystallography confirmed that the $[PPh_4]^+$ salt was isomorphous with the previously studied $[AsPh_4]^+$ salt[26] and that the crystal faces were normal to the unit cell axes with the tetragonal uniaxis (and molecular z axis) often, but not always, the long axis of the crystal. Crystals could be oriented using polarized light, as a marked dichroism makes the crystals light green when $E \parallel c$ and dark green when $E \perp c$. Single-crystal specimens for polarized absorption studies were mounted with the 001 or 100 face flush on a quartz disk and secured with an optically transparent resin (Crystalbond). The specimen was polished to the desired thickness (~90 μm for xy polarization and ~240 μm for z polarization) using successively finer lapping film and then masked off with black electrical tape. Mull samples were prepared by finely grinding fresh crystals in a Wiggle-bug apparatus within a drybox, dispersing the solid in dried fluorolube and sealing the mull between quartz disks.

$[AsPh_4][MoOCl_4(H_2O)]$. The aquo adduct was synthesized and crystals grown as for the five-coordinate compound above, except undried CH_2Cl_2 was used. These crystals are isomorphous with the five-coordinate complex,[27] but do not behave tetragonally with respect to polarized light. Under crossed polarizers the *ab* face does not completely extinguish, and a large CD signal is found when measured normal to this face. Single-crystal specimens were prepared as above using the *bc* faces which showed extinction directions parallel to crystal edges. Mull specimens were finely ground in air, dispersed in polydimethylsiloxane, and pressed between quartz disks.

$[NH_4][MoOCl_4(H_2O)]$. Solutions were prepared by dissolving $(NH_4)_2[MoOCl_5]$[28] in concentrated HCl solution;[29] glycerin (50% by volume) was added to aid glassing and produced no change in absorption or EPR spectra.

(13) Jørgensen, C. K. *Acta Chem. Scand.* **1957**, *11*, 73-85.
(14) Gray, H. B.; Hare, C. R. *Inorg. Chem.* **1962**, *1*, 363-368.
(15) Hare, C. R.; Bemal, I.; Gray, H. B. *Inorg. Chem.* **1962**, *1*, 831-835.
(16) Collison, D. *J. Chem. Soc., Dalton Trans.* **1990**, 1-6.
(17) Johnson, M. K. In *Metal Clusters in Proteins*; Que, L., Ed.; ACS Symposium Series 372; American Chemical Society: Washington, DC, 1988; pp 326-342.
(18) Stephens, P. J. *Annu. Rev. Phys. Chem.* **1974**, *25*, 201-232.
(19) Sutherland, J. C.; Holmquist, B. *Annu. Rev. Biophys. Bioeng.* **1980**, *9*, 293-326.
(20) Piepho, S. B.; Schatz, P. N. *Group Theory in Spectroscopy with Applications to Magnetic Circular Dichroism*; Wiley-Interscience: New York, 1983.
(21) Peterson, J.; Godfrey, C.; Thomson, A. J.; George, G. N.; Bray, R. C. *Biochem. J.* **1986**, *233*, 107-110.
(22) Johnson, J. L.; Bastian, N. R.; Rajagopalan, K. V. *Proc. Natl. Acad. Sci. U.S.A.* **1990**, *87*, 3190-3194.
(23) Benson, N.; Farrar, J. A.; McEwan, A. G.; Thomson, A. J. *FEBS Lett.* **1992**, *307*, 169-171.
(24) Finnegan, M. G.; Hilton, J.; Rajagopalan, K. V.; Johnson, M. K. *Inorg. Chem.* **1993**, *32*. 2616-2618.
(25) Cleland, W. E., Jr.; Barnhardt, K. M.; Yamanouchi, K.; Collison, D.; Mabbs, F. E.; Ortega, R. B.; Enemark, J. H. *Inorg. Chem.* **1987**, *26*, 1017-1025.
(26) Garner, C. D.; Hill, L. H.; Mabbs, F. E.; McFadden, D. L.; McPhail, A. T. *J. Chem. Soc., Dalton Trans.* **1977**, 853-858.
(27) Garner, C. D.; Hill, L. H.; Mabbs, F. E.; McFadden, D. L.; McPhail, A. T. *J. Chem. Soc., Dalton Trans.* **1977**, 1202-1207.
(28) Saha, H. K.; Banerjee, A. K. *Inorg. Synth.* **1974**, *15*, 100.
(29) Boorman, P. M.; Garner, C. D.; Mabbs, F. E. *J. Chem. Soc., Dalton Trans.* **1975**, 1299-1306.

LMoO(OCH_2CH_2O) was prepared according to literature methods.[25] The glassing solution used was 2:1 dichloroethane/DMF; the mulling agent was fluorolube.

LMoO(catecholate) was prepared according to literature methods,[25] and absolute ethanol was used as the glassing solution.

LMoOCl_2 was prepared according to literature methods,[25] and 1:3 dichloroethane/DMF was used as the glassing solution. The mulling agent was mineral oil.

LMoO(SCH_2CH_2S) was prepared according to literature methods,[25] and 50:50 toluene/DMF was used as the glassing solution. The mulling agent was mineral oil.

LMoO(toluene-3,4-dithiolate) was prepared according to the literature method.[25] The mulling agent was mineral oil.

2. Absorption and MCD Spectral Studies. Single-Crystal Polarized Absorption Spectra. Polarized absorption spectra were measured on a MacPherson RS-10 double beam spectrometer described previously,[30] but with upgraded electronics. A pair of Glan-Taylor polarizers matched from 2000 to 25000 Å were used in the sample and reference beams. Two gratings blazed at 3000 and 7500 Å were used to cover the spectral regions. An extended S-20 photomultiplier tube covered the region from 2200 to 8000 Å and a dry-ice cooled S-1 tube covered 5000 to 10000 Å. Variable-temperature experiments from 300 to 4.2 K were done with a Janis Super-Vari Temp Dewar.

Room Temperature Mull and Solution Absorption Spectra. Absorption spectra of mulls and solutions at room temperature were obtained on an OLIS 4300S modified Cary 14 UV/vis/near-IR spectrophotometer.

Magnetic Circular Dichroism Spectra. MCD spectra in the 2500 to 8500 Å region were collected on a JASCO J-500C CD spectropolarimeter configured with focusing optics and an Oxford SM4 cryostat/superconducting magnet capable of producing fields up to 6.0 T and sample temperatures down to 1.5 K. For the 6000 to 20000 Å region, MCD spectra were collected on a JASCO J-200 CD spectropolarimeter configured with focusing optics and an Oxford cryostat/superconducting magnet capable of producing fields up to 7.0 T and sample temperatures down to 1.5 K. Crystalline samples were prepared as described above; mull samples were finely ground and dispersed in one of three optically transparent mulling agents and then sandwiched between quartz disks. Glasses were prepared by injecting ~0.25 mL of the compound dissolved in an appropriate glassing solvent into a cell comprised of two quartz disks sandwiching a rubber o-ring of thickness 2 mm. Depolarization of the beam was checked for each sample by measuring the CD spectrum of a standard nickel (+)-tartrate solution with the sample positioned in the beam path both before and after the standard.[20] Samples which decreased the CD signal by less than 10% were considered suitable. Unless otherwise noted all MCD spectra were obtained at magnetic fields of 5 T and at stable (±0.2 K) temperatures between 4.2 and 6 K.

3. Theoretical Calculations. Computations. Molecular orbital calculations were performed utilizing the nonempirical Fenske–Hall program[31] (Version 5.0) with the default basis functions provided. Computations were performed on a clustered Vaxstation 3100.

Structures. Geometries for compounds were taken from crystal structures or were built up from average bond distances and angles as determined by a search of the Cambridge Structural Database. In each case, the geometry was idealized to the highest appropriate symmetry of C_{4v}, C_{2v}, or C_s. No substantial differences were found for compounds run in both idealized geometry and from crystal structure coordinates.

III. Results for $[MoOCl_4]^-$ and $[MoOCl_4(H_2O)]^-$

Overall, six features common to both $[MoOCl_4]^-$ and $[MoOCl_4(H_2O)]^-$ have been observed in the following spectra which we will refer to as bands 1–6 in increasing energy order. The electronic structures of the $[MoOCl_4]^-$ and $[MoOCl_4(H_2O)]^-$ anions in solid, glass, and solution samples are expected to be very similar, but some differences in peak position and shape are observed between phases (*vide infra*). All MCD features show an inverse dependence of intensity on temperature and a linear dependence on the magnetic field strength, with no sign of saturation at 5 T. This magnetic field dependence is consistent with all absorbencies originating from species with one unpaired electron having an isotropic g value of approximately 2.0.

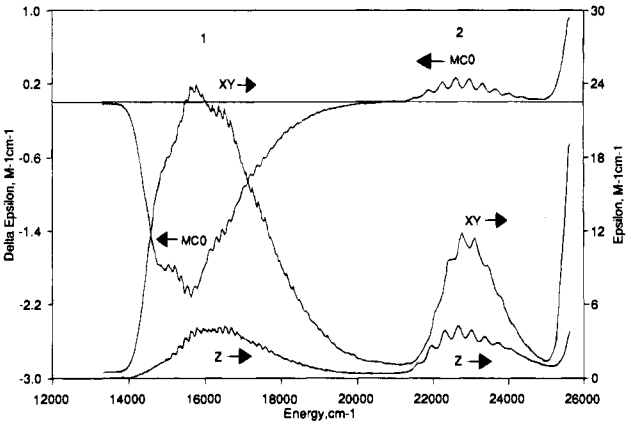

Figure 2. Single-crystal xy-, and z-polarized absorption and MCD spectra of $[PPh_4][MoOCl_4]$ at 4.2 K. The MCD spectrum was obtained at a field strength of 0.5 T. The xy-polarized spectrum has been offset +0.5 units to prevent overlap.

Figure 2 shows the 5 K polarized single-crystal absorption and single-crystal MCD spectra for $[PPh_4][MoOCl_4]^-$ in the region 12000–26000 cm^{-1}. The z-polarized spectrum shows two broad bands with $\epsilon = 4\ M^{-1}\ cm^{-1}$. The broad band in the 14000–19000 cm^{-1} region (band 1) shows multiple convoluted vibrational progressions including those of approximately 900 and 170 cm^{-1} without a clear origin; the band starting at 21615 cm^{-1} (band 2) shows a single vibrational progression of 351 cm^{-1}. Neither z-polarized band shows any temperature dependence other than slight broadening. The xy-polarized spectrum shows a broad asymmetric band from 14000–20000 cm^{-1} that resembles that of the z-polarized spectrum. However, the xy-polarized band is more intense ($\epsilon = 23\ M^{-1}\ cm^{-1}$) due mainly to the unstructured component at low energy. The overall vibrational structure is not as pronounced as in z polarization, but appears to be identical to that in the z-polarized spectrum. This band shows noticable broadening on the low-energy side as the temperature is increased from 5 K to room temperature, but no substantial increase in oscillator strength. The band at ca. 23000 cm^{-1} is also more intense in xy polarization ($\epsilon = 12\ M^{-1}\ cm^{-1}$), but the vibrational structure of the band is less well resolved. Inspection of the first derivative of the band shape indicates that two different progressions are present; one of which is identical to that found in the z-polarized spectrum, the other beginning about 110 cm^{-1} to higher energy and having a slightly smaller energy spacing of 340 cm^{-1}. This peak shows substantial temperature dependence, and the integrated intensity decreases by 50% upon cooling from room temperature to 5 K. These features of the spectra have been previously reported[26,32] with various amounts of detail.

The single-crystal MCD spectrum of $[MoOCl_4]^-$ has not been previously reported. In the charge transfer region of cubic Cs_2ZrCl_6 doped with Mo^{4+} the related $[MoOCl_5]^-$ ion (Mo^{5+}) has been identified as an impurity through its temperature-dependent MCD,[33] but no explanation of the spectra has been given. The orientation appropriate for collection of single-crystal MCD of $[PPh_4][MoOCl_4]$ is with light propagated along the tetragonal

(30) Wilson, R. B.; Solomon, E. I. *Inorg. Chem.* **1978**, *17*, 1729.
(31) Hall, M. B.; Fenske, R. F. *Inorg. Chem.* **1972**, *11*, 768.
(32) Winkler, J. R.; Gray, H. B. *Comments Inorg. Chem.* **1981**, *1*, 257–263.
(33) Collingwood, J. C.; Schwartz, R. W.; Schatz, P. N.; Patterson, H. H. *Mol. Phys.* **1974**, *27*, 1291–1317.

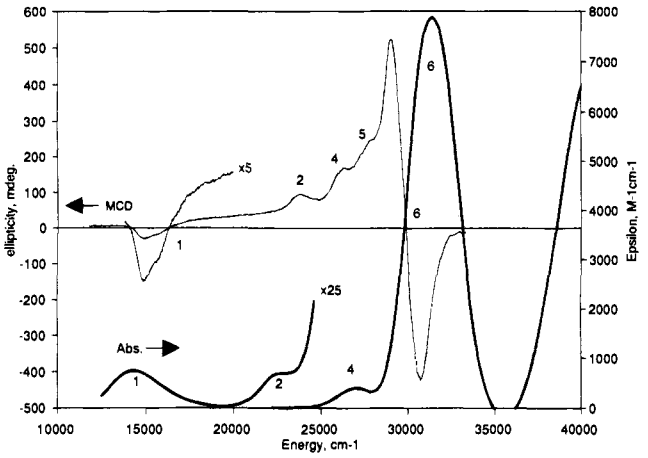

Figure 3. Room temperature solution absorption (bold line) and 5 K mull MCD (thin line) spectra of $[PPh_4][MoOCl_4]$.

uniaxis, which corresponds to the *xy*-polarized molecular absorption spectrum. A striking feature of this MCD spectrum (Figure 2) for the ligand field transitions is the strongly negative asymmetric feature (band 1) near 16000 cm^{-1} and the complete absence of any positive MCD intensity in this region, in contrast to the mull and glass spectra described below. The peak has an extreme at 15780 cm^{-1} as does the *xy*-polarized absorption band, but the shoulders at ca. 15000 and 16500 cm^{-1} switch relative intensity giving them slightly different band shapes. The vibrational fine structure observed appears to be identical to that found in both the *xy* and *z* polarizations. Band 2 at 23000 cm^{-1} shows a positive MCD and the same vibrational fine structure as the *z*-polarized absorption spectrum.

Figure 3 shows the room temperature dichloromethane solution absorption and 5 K mull MCD spectra of the five-coordinate $[MoOCl_4]^-$ ion in the region from 10000 to 35000 cm^{-1}. The solution spectra are similar to those reported previously[26] showing two weak absorption peaks at 14300 (band 1) and 22900 (band 2) cm^{-1} and two intense peaks at 26900 (band 4) and 31400 (band 6) cm^{-1}. The mull MCD spectrum is in accord with that recently independently described by Sabel and Gewirth.[34] The mull MCD spectrum of $[MoOCl_4]^-$ shows a weak negative peak at ca. 15000 cm^{-1} followed by a weaker positive signal (both making up band 1). The weak positive signal extends into the higher energy bands at ca 23000 cm^{-1} where three distinct features are observed (positive (band 2) at 23800, positive (band 4) at 26300, and an inflection (band 5) at 28000 cm^{-1}) on the low energy side of a very strong positive/negative pair of peaks (both making up band 6) crossing at 30000 cm^{-1}. The crossing point for this feature is not identical with the solution absorption maxima of band 6; this variation is attributed to the differing phases for the two measurements. The absorption spectrum does not show any bands in the region of ca. 20000 cm^{-1}. The "sloping background" in the MCD of this region shows the same temperature and magnetic field dependencies as the rest of the spectrum and is independent of mulling agent, cation, and concentration. This MCD feature might arise from the presence of a small fraction of perturbed complex which is formed during mulling.

Figure 4 (top) shows the 5 K polarized single-crystal absorption and mull MCD spectra for $[AsPh_4][MoOCl_4(H_2O)]$. The low-energy region (band 1) shows similar characteristics to the five-coordinate species (band 1), but the vibrational structure is much more clearly resolved. In an earlier examination,[27] only a single progression of ca. 760 cm^{-1} was observed in *xy* polarization. Here, band 1 clearly contains two different components, both displaying fine structure. The higher energy component is observed in both *xy* and *z* polarization, whereas the lower energy component is only visible in *xy* polarization. Figure 4 (bottom) presents an expanded view of the low energy band (band 1) of $[MoOCl_4(H_2O)]^-$ detailing the major vibrational progressions of 860 and 178 cm^{-1} built on both the *xy*- and *z*-polarized origins. In *z* polarization the single band origin is at 12658 cm^{-1}. Progressions identical in energy to those found in the *z*-polarized spectrum are present in the *xy*-polarized spectrum convoluted with an identically shaped, but more intense band envelope starting 810 cm^{-1} lower in energy (11848 cm^{-1}). The mull MCD of band 1 displays a progression of minima with a separation of approximately 900 cm^{-1}. The minima coincide with maxima in the *xy*-polarized absorption spectra. At ca. 23000 cm^{-1}, band 2 is visible in both polarizations and shows a 350 cm^{-1} progression in *z* polarization. The positive MCD intensity of band 2 is markedly decreased compared to the five-coordinate complex by a new overlapping transition of opposite sign. That new feature, band 3 at 24200 cm^{-1}, is only observed in *xy* polarization. The large baseline in the *xy*-polarized spectra prevented quantitative examination for fine structure or temperature dependence, due to light limitations above 23000 cm^{-1}; however, the *xy*-polarized absorption intensity does increase with increasing temperature in this region.

Figure 5 shows the room temperature absorption and 5 K MCD spectra for $[NH_4][MoOCl_4(H_2O)]$ in a glass of concentrated HCl and glycerin between 10000 and 40000 cm^{-1}. The spectra are similar to those obtained for the mull (Figure 4) but more clearly present the individual peaks due to the elimination of the MCD "sloping background" at ca. 20000 cm^{-1}. An additional peak is visible at 25000 cm^{-1} due to the presence of an impurity resulting from corrosion of the syringe needle during the few seconds that it takes to inject the highly acidic solution into the sample cell. In samples with differing concentrations, only the relative intensity of this peak changed. The primary features of the MCD are a negative–positive pair (negative more intense) crossing at 14700 cm^{-1} (band 1), a weak positive peak (band 2) at 22900 cm^{-1}, an intense positive peak (band 4) at 28000 cm^{-1}, and an intense positive–negative pair (band 6) crossing at 32100 cm^{-1}. In the absorption spectra peak maxima occur at 14000 (band 1), 22600 (band 2), 28000 (band 4), and 32200 (band 6) cm^{-1}.

IV. Analysis Of $[MoOCl_4]^-$ and $[MoOCl_4(H_2O)]^-$ Data

1. Molecular Orbital Calculations and Selection Rules. Figure 6 presents a selected portion of the DVXα molecular orbital calculations of Deeth[35] for $[MoOCl_4]^-$. Of the multitude of theoretical studies performed on these systems, Deeth's DVXα treatment best accounts for the experimental results. It gives pertinent orbital origins, symmetry, and ordering information for assignment of the electronic absorption and MCD spectra of the $[MoOCl_4]^-$ and $[MoOCl_4(H_2O)]^-$ ions. Both may be treated with the same C_{4v} molecular orbital scheme because H_2O acts primarily as an axial σ donor whose orbitals appear lower in energy than those of the equatorial chlorine atoms.[35] The diagram shows the molecular orbitals of interest arising from interaction of the Cl π orbitals and the Mo d orbitals in C_{4v} symmetry. The d_{xy} orbital ($2b_2$) is singly occupied and the ground state is $^2B_2$ which has been confirmed experimentally.[16] The chlorine-based in-plane $1b_2$ orbital is involved in Mo–Cl bonding and occurs at lower energy. $^2B_2$ to ^2E transitions are electric dipole allowed (with *x,y* polarization) in C_{4v} symmetry.

(34) Sabel, D. M.; Gewirth, A. A. *Inorg. Chem.* **1994**, *33*, 148.

(35) Deeth, R. J. *J. Chem. Soc., Dalton Trans.* **1991**, 1895–1900.

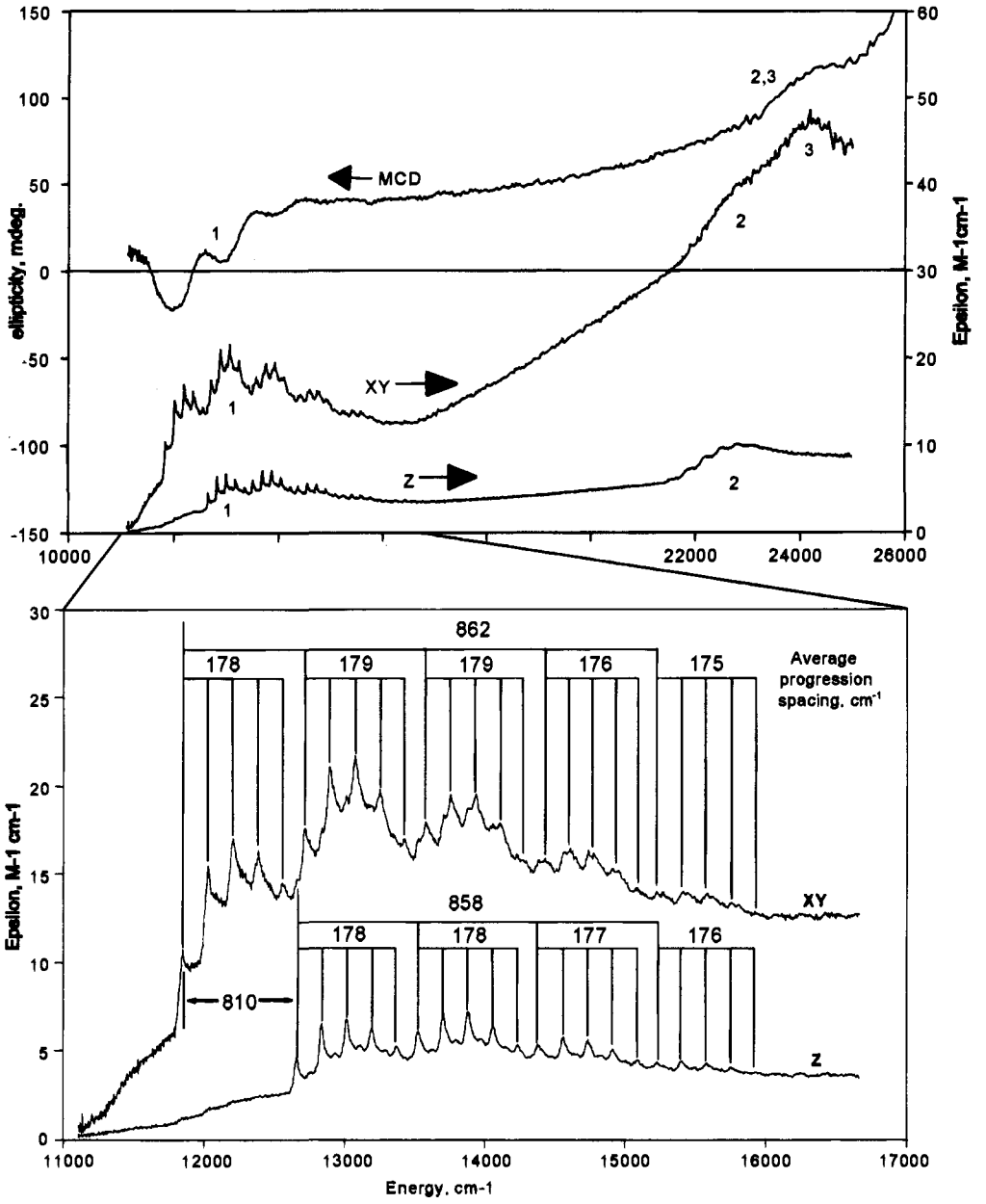

Figure 4. (Top) Single-crystal xy- and z-polarized absorption and mull MCD spectra of $[AsPh_4][MoOCl_4(H_2O)]$ at 4.2 K. The MCD spectrum was obtained at a magnetic field strength of 5 T. (Bottom) Expanded view of the lowest energy band of the polarized absorption spectra showing the separation of the major vibrational progressions and the spin–orbit splitting of the excited state.

This includes the primarily d–d transition from d_{xy} to $d_{xz,yz}$ and the charge transfer transition from Cl π orbitals of e symmetry to the half occupied metal d_{xy} orbital.

Inclusion of spin–orbit coupling (ca. 900 cm^{-1} for Mo^{5+} [36] and −587 cm^{-1} for chloride[37]) leads to a relaxation of these selection rules and splitting of the orbitally degenerate E sets, as shown in the state diagram (Figure 7). In Figure 7, the ordering of states is determined by the assignments below, rather than the energies of the molecular orbital calculations in Figure 6. In C_{4v}' symmetry, the ground state is Γ_7. The ^2E states will be split into two spin–orbit components, Γ_7 and Γ_6 separated by approximately the spin–orbit coupling constant of the atom(s) upon which the transition is centered.[16] Because chloride and molybdenum have oppositely signed many-electron spin–orbit coupling constants, the Γ_6 state will lie lower in energy for the $d_{xy} \rightarrow d_{xz,yz}$ ligand field transition (band 1), whereas the Γ_7 state will lie lower in energy for the charge transfer transitions from chlorine π orbitals of e symmetry to d_{xy} (bands 5 and 6). The effects of spin–orbit coupling make $\Gamma_7 \leftarrow \Gamma_7$ transitions allowed in z polarization, and both $\Gamma_7 \leftarrow \Gamma_7$ and $\Gamma_6 \leftarrow \Gamma_7$ transitions allowed in x,y polarization. Temperature-dependent vibrational mechanisms can also provide an intensity source which relaxes the C_{4v} selection rules. An E vibrational mode can make $^2A_1 \leftarrow {}^2B_2$ and $^2B_1 \leftarrow {}^2B_2$ vibrationally allowed in xy polarization and $^2E \leftarrow {}^2B_2$ in z polarization. The Zeeman perturbation of an external magnetic field along the molecular z axis lowers the effective symmetry to C_4'. The right side of Figure 7 shows the resulting splitting diagram and the predicted signs for the low-temperature MCD transitions due to C terms in this orientation. At 4.2 K and 5 T the lower energy component of this Kramers doublet (Γ_7) will contain approximately 83% of the unpaired electron population. We will utilize the C_{4v} nomenclature, appending the C_{4v}' double group Γ notation as needed. The C_4' notation

(36) Figgis, B. N. *Introduction to Ligand Fields*; John Wiley & Sons, Inc: New York, NY, 1966, p 60.

(37) Kon, H.; Sharpless, N. E. *J. Phys. Chem.* **1966**, *70*, 105–111.

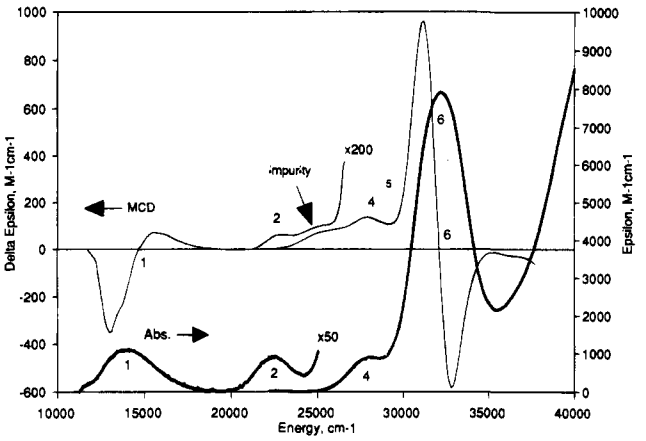

Figure 5. Room temperature solution absorption (bold line) and 5 K glass MCD (thin line) of $[NH_4][MoOCl_4(H_2O)]$ in 50/50 concentrated HCl/glycerin.

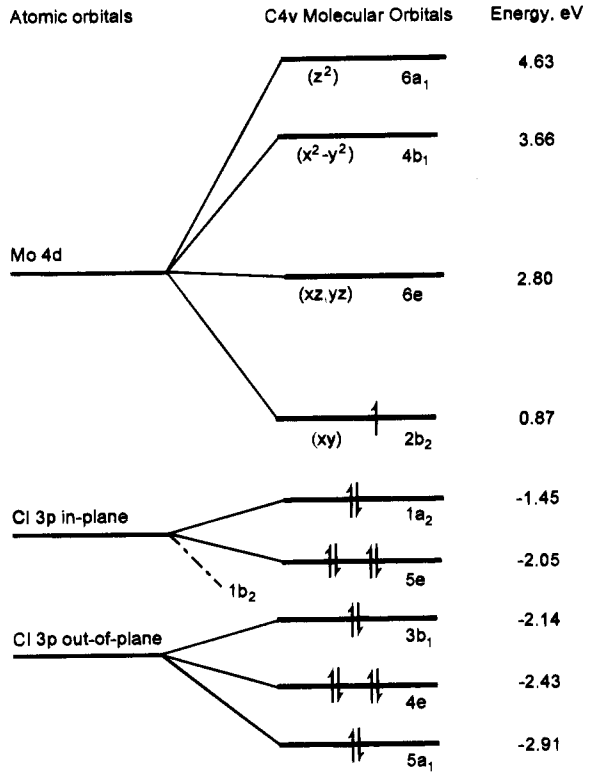

Figure 6. Molecular orbital energy level diagram for $[MoOCl_4]^-$. Energy values taken from ref 35.

is used at this point only in determining the sign of the dominant low temperature MCD transition. In C_4', $\Gamma_5 \leftarrow \Gamma_7$ (and $\Gamma_6 \leftarrow \Gamma_8$) transitions are right circularly polarized (negative), while $\Gamma_7 \leftarrow \Gamma_7$ (and $\Gamma_8 \leftarrow \Gamma_8$) transitions are left circularly polarized (positive).

While this group theoretical approach results in linearly and circularly polarized selection rules, it provides no information about intensity of the transitions. Fully allowed as well as spin–orbit or vibronically allowed ligand field transitions are expected to be uniformly weak ($\epsilon < 100\ M^{-1}\ cm^{-1}$), while charge transfer transitions will vary widely in intensity depending on metal–ligand overlap.[38] Charge transfer transitions to d_{xy} from ligand orbitals in the equatorial plane are expected to have larger ϵ values than those from out-of-plane ligand orbitals due to simple

(38) Solomon, E. I. *Comments Inorg. Chem.* **1984**, *3*, 227–320.

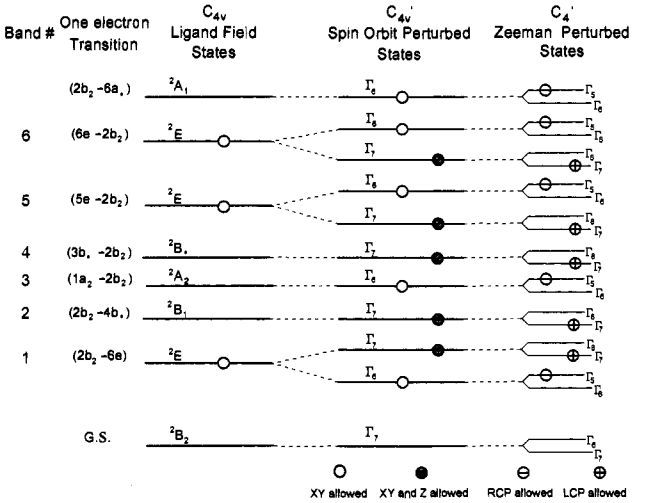

Figure 7. State diagram for $[MoOCl_4]^-$ including spin–orbit and Zeeman perturbations and showing polarized light absorption selection rules.

overlap considerations.[39] The reverse intensity relationship is expected for charge transfer transitions to the d_{xz},d_{yz} set.

In general, MCD intensities for individual components will scale with the intensity of the corresponding absorption peak (however, overlap of transitions tends to obscure this). The two in-state spin–orbit split components of the E levels should give rise to two temperature-dependent MCD bands with equal intensity and opposite sign. If the splitting of these components is less than the bandwidth, they are expected to overlap producing a derivative shaped feature called a pseudo-*A* term[20] whose crossing point corresponds to the absorption band maxima. From Figure 7, the ligand field $^2E \leftarrow {}^2B_2$ pseudo-*A* is expected to be positive (the sign of its higher energy component is positive) while the Cl charge transfer pseudo-*A* terms are expected to be negative. If spin–orbit coupling effects are small, then E states typically show temperature-independent A terms of opposite sign to that observed due to *C* terms. This has been observed in the case of high symmetry compounds of the vanadyl group[40] in which spin–orbit splitting of the ligand field E is only $\sim 150\ cm^{-1}$. Such a temperature-independent contribution was not observed in these Mo compounds, and we have analyzed the MCD results as arising from *C* terms only.

The expressions relating MCD *C* term intensity to electronic structure have been given elsewhere.[20] *C* term intensity requires transition moments in two perpendicular directions and is proportional to the product of the individual transition dipole moments (m_i $i = x, y, z$) and the ground state **g** tensor components (g_i $i = x, y, z$), as shown in eq 1. In the oriented single-crystal spectrum, with light propagated along the z molecular axis, the molecule is oriented such that only the first term is nonzero. Since the x- and y-polarized transitions are nearly an order

$$C_0 \propto \mathbf{g}\cdot(m\times m) = g_z m_x m_y + g_y m_x m_z + g_x m_y m_z \qquad (1)$$

of magnitude more intense than those in z, this term should dominate the MCD spectra, even in orientationally averaged cases where the other two terms also contribute.

2. Band Assignments. Band 1 is assigned to the $^2E \leftarrow {}^2B_2$ ligand field transition in accord with previous assignments.[16,26,32] The featureless low-energy side of the band in the *xy*-polarized

(39) Lever, A. B. P. *Inorganic Electronic Spectroscopy*, 2nd ed.; Elsevier Science Publishing: New York, 1986, p 241.

(40) Robbins, D. J.; Stillman, M. J.; Thomson, A. J. *J. Chem. Soc., Dalton Trans.* **1974**, 813–820.

single-crystal absorption spectrum of $[MoOCl_4]^-$ at ca. 15000 cm^{-1} (Figure 2) and the structured progression in $[MoOCl_4(H_2O)]^-$ starting at 11848 cm^{-1} (Figure 4) are assigned to the $^2E(\Gamma_6) \leftarrow {}^2B_2(\Gamma_7)$ component that is *xy* allowed but *z* forbidden (Figure 7). The structured portion of the band in both *xy*- and *z*-polarized spectra of $[MoOCl_4]^-$ (ca. 16000 cm^{-1}) and the structured progression in $[MoOCl_4(H_2O)]^-$ starting at 12658 cm^{-1} are assigned to the $^2E(\Gamma_7) \leftarrow {}^2B_2(\Gamma_7)$ component. The separation between the two component band envelopes in $[MoOCl_4]^-$ is approximately 800 cm^{-1}, and the vibronic origins in $[MoOCl_4(H_2O)]^-$ (Figure 4) are clearly separated by 810 cm^{-1}. Both values are reasonable for the Mo(V) spin–orbit splitting of the e ($d_{xz,yz}$) orbitals. The values are smaller than that of the free ion, in accord with the expected reduction due to covalent bonding to the terminal oxo group.

For both the five- and six-coordinate complexes the single-crystal absorption spectra show extensive fine structure on this ^2E band. While similar, the progressions are most clearly resolved in the spectra of the six-coordinate complex (Figure 4). The excited-state vibrational progressions of 860 and 178 cm^{-1} are respectively assigned to the totally symmetric Mo=O stretch (1008 and 985 cm^{-1} in the ground state of the five- and six-coordinate complexes, respectively)[27] and the totally symmetric O=Mo–Cl bend (184 cm^{-1} in the ground state of the five-coordinate complex).[44] The large reduction in the excited state molybdenum–oxo stretching frequency is attributable to the electronic excitation of moving an essentially nonbonding electron into an orbital that is antibonding with respect to the molybdenum–oxo π bond, thus weakening the bond. In the six-coordinate complex the bond is further weakened by the competitive bonding of the axial ligand.

For both $[MoOCl_4]^-$ and $[MoOCl_4(H_2O)]^-$, the orientationally averaged mull and glass MCD spectra of band 1 show a sharply negative absorbance followed by weak positive absorbance. Fine structure is weakly observed for $[MoOCl_4]^-$ and strongly observed for $[MoOCl_4(H_2O)]^-$, as in the single-crystal absorption cases. The lower energy feature appears to be the negative component of the pseudo-*A* term that is expected for an ^2E ligand field transition. However, the *single-crystal* MCD of $[MoOCl_4]^-$ (Figure 2) shows only a single asymmetric negative MCD for the ^2E transition. No positive MCD intensity is observed in this region. Comparison of the band shapes for these transitions as measured in the single-crystal MCD spectrum and in the identically oriented *xy* linearly polarized spectrum reveal that a positive contribution, as expected for the $^2E(\Gamma_7) \leftarrow {}^2B_2(\Gamma_7)$, is present, but that the $^2E(\Gamma_6) \leftarrow {}^2B_2(\Gamma_7)$ transition is more intense. This leads to the difference in relative intensities between the shoulders of this band. Quantitative simulation of the *xy*-polarized spectrum of the six-coordinate complex using the band shape of the *z*-polarized spectrum indicates that the two components have identical band shapes and that the lower energy Γ_6 component is twice as intense as the Γ_7 component. A similar ratio of intensities is apparent in the single-crystal spectrum of the five-coordinate complex. The sum of the intensities from these two components should give the band shape of the absorption spectrum, whereas the difference should give the band shape of the MCD spectrum which is found in the simulations. The significant difference in intensity of these two components accounts for the completely negative MCD peak in the single-crystal spectrum of the five-coordinate complex. The greater intensity of the Γ_6 leads to its vibrational progressions being observable over a larger energy range which extends to higher energy than those of the Γ_7 transition in the high energy tail of this band (i.e. the Γ_7 component fits completely within that of the Γ_6 component). That effect is countered in orientationally averaged samples because the Γ_6 transition is not allowed in *z* polarization; it will lose absorption intensity for molecules rotated from a parallel (*xy*) orientation into a perpendicular (*xz* or *yz*) orientation. Substituting experimental transition moments (taken as the square root of the band maximum ϵ in Figure 4), eq 1 predicts that the ratio of *C* term intensity for Γ_6 vs Γ_7 in the *xy* orientation should be 2:1 (as found for the components in the *xy*-polarized spectrum), while for an orientationally averaged sample (each term contributing one-third) it would be approximately 0.8:1. In the orientationally averaged situation (Figures 3–5), positive MCD should be observed in the high-energy tail of the band because the Γ_6 component will no longer completely obscure the Γ_7 component and, in fact, the Γ_7 will be the larger contributor in the region where they overlap.

The origin of the difference in intensity of the two components of the spin–orbit split ^2E transition is reasonably ascribed to out-of-state spin–orbit coupling of the Γ_7 with other nearby Γ_7 states (Figure 7). When only in-state spin–orbit coupling is considered, the two components should have equal intensities and oppositely signed MCD.[41] Out-of-state spin orbit coupling within the d manifold[42] can account for approximately 1% of the intensity difference. Thus, the major contribution to this difference must arise from coupling with ligand based states (*vide infra* band 4). Gerstman and Brill[43] have shown how such an out-of-state spin–orbit mechanism including ligand-based states can produce large differences in the intensity of MCD transitions in cupric compounds.

Band 2 is observed at ca. 23000 cm^{-1} in each of the spectra; it has previously[16,32] been assigned to the $d_{xy} \rightarrow d_{x^2-y^2}$ transition based on its polarization, vibronic structure and energy shifts when equatorial ligands are changed. These MCD results further confirm those findings and allow for separation of the spin orbit and vibronic contributions to its *xy* intensity. The single-crystal MCD spectrum of $[MoOCl_4]^-$ shows a band whose positive sign is consistent with the $^2B_1(\Gamma_7) \leftarrow {}^2B_2(\Gamma_7)$ transition. Its vibrational progression of 351 cm^{-1} parallels the temperature-independent progression observed in the *z*-polarized single-crystal absorption spectrum of both $[MoOCl_4(H_2O)]^-$ and $[MoOCl_4]^-$. This progression is most reasonably assigned to the a_1 Mo–Cl stretch in the excited state. The ground-state energy for this vibration[44] is 354 cm^{-1} in $[MoOCl_4]^-$. This excited-state distortion is consistent with the $d_{xy} \rightarrow d_{x^2-y^2}$ assignment which transfers a nonbonding e^- to an orbital that is σ antibonding with respect to the chlorides. The totally symmetric progression is built upon an allowed origin, the consequence of spin–orbit coupling involving this state, as no vibrational modes will enable *z* intensity for this transition. In the temperature dependent *xy*-polarized band 2 of $[MoOCl_4]^-$, the first progression is identified as the same spin–orbit allowed progression in the a_1 Mo–Cl stretch as seen in *z* polarization and the single-crystal MCD. This component should be temperature independent. The temperature dependence of this *xy*-polarized band arises because vibronic intensity can be acquired in *xy* polarization via an enabling mode of e symmetry, and such a mode is the most reasonable assignment of the origin of the second progression identified. The antisymmetric Mo–Cl bend of e symmetry[44] occurs at 114 cm^{-1} in $[MoOCl_4]^-$.

Band 3, observed here only in the single-crystal absorption spectrum of $[MoOCl_4(H_2O)]^-$, is assigned to the $^2A_2(\Gamma_6) \leftarrow$

(41) Westmoreland, T. D.; Wilcox, D. E.; Baldwin, M. J.; Mims, W. B.; Solomon, E. I. *J. Am. Chem. Soc.* **1989**, *111*, 6106–6123.
(42) Reference 39, p 177.
(43) Gerstman, B. S.; Brill, A. S. *J. Chem. Phys.* **1985**, *82*, 1212–1230.
(44) Collin, R. J.; Griffith, W. P.; Pawson, D. *J. Mol. Struct.* **1973**, *19*, 531–544.

$^2B_2(\Gamma_7)$ charge transfer transition. This transition, which is symmetry forbidden in C_{4v}, becomes allowed via spin–orbit coupling. Neither the lower symmetry perturbation of the axial ligand (to C_{2v}) or coupling to a vibrational mode (no a_2 normal modes) can explain the observation of intensity in xy, but not z, polarization. That observation confirms a $\Gamma_6 \leftarrow \Gamma_7$ transition. The weaker positive MCD intensity of band 2 in $[MoOCl_4(H_2O)]^-$ compared to $[MoOCl_4]^-$ is presumably due to overlap with this negatively signed transition. This weakly absorbing transition has been observed previously in polarized single-crystal spectra of $[MoOCl_4(H_2O)]^-$ and $[MoOCl_4(CH_3OH)]^-$ and was suggested to have arisen from a transition internal to the molybdenyl fragment.[27] We assign this band to the charge transfer transition from the chloride a_2 orbital for three reasons: (a) the energy corresponds to that in Deeth's molecular orbital calculations;[35] (b) Jørgensen's empirical principle of optical electronegativity[45] predicts that for a given metal the first charge transfer transition from the oxygen p orbitals of water will occur at least 15000 cm^{-1} above the first chloride charge transfer transition[46] and those from an oxide even higher; (c) the absence of any similar band in $[MoOCl_4]^-$ or other molybdenyl compounds rules out a ligand field transition to d_{z^2}.

Band 4 is assigned as the chloride charge transfer $^2B_1 \leftarrow {}^2B_2$ (Figure 7). The single positive peak in the MCD indicates a $\Gamma_7 \leftarrow \Gamma_7$ transition. The absorption intensity of 600 M^{-1} cm^{-1} is typical of an orbitally forbidden charge transfer transition gaining intensity through a spin–orbit or vibronic mechanism.[47] Further support for this assignment is the requirement of a B_1 charge transfer state to be close in energy to the ground state in the theoretical interpretation of the inverted ($g_\parallel > g_\perp$) EPR parameters of molybdenyl compounds[37] via out-of-state spin–orbit coupling. Sabel and Gewirth propose this assignment[34] and calculate reasonable EPR parameters from their MCD derived transition energies.

Band 5 is the weak negative pseudo-A feature at 28000 cm^{-1} in the mull MCD of $[MoOCl_4]^-$ that indicates a transition involving orbitals of e symmetry. The molecular orbital calculations (Figure 6) place two E states in this energy range. The low absorption intensity in this region indicates poor overlap. Consequently we assign this feature to the $^2E \leftarrow {}^2B_2$ transition arising from charge transfer from out-of-equatorial-plane chloride $p\pi$ orbitals of e symmetry to d_{xy}.

Band 6 is the intense negative pseudo-A feature centered about 30000 cm^{-1} that can be assigned to the $^2E \leftarrow {}^2B_2$ charge transfer transition from the in-plane Cl π orbitals of e symmetry to the d_{xy} orbital of the metal. The large absorption intensity is consistent with the large overlap expected between the d_{xy} orbital and these in-plane chloride orbitals, and the energy agrees with the calculations of Deeth[35] (Figure 6).

V. Results for $LMoOX_2$ Complexes

1. Spectra. The absorption and MCD spectra of a series of $LMoOX_2$ complexes (Figure 1b) with X = O, Cl, and S donor atoms are depicted in Figures 8–12. All of the complexes give rich MCD spectra that show temperature and field dependence indicative of C terms arising from an approximately $g = 2.0$ species. MCD spectra of mulled solids and glassed solutions were obtained for each compound. The quantitative glass spectrum is shown unless the EPR spectrum or the mull MCD spectrum have indicated a change in structure in the glassed solution. The MCD spectrum measured in each phase is qualitatively the same, but depolarization effects are greater in the mull samples and impurity effects due to grinding produce some deviations in the baseline position and relative band intensity. Both mull and glass spectra of $LMoOCl_2$ (Figure 10) are shown to illustrate the changes between phases, which were largest for this complex. Since the deconvolution of individual features becomes more model dependent as the number of overlapping transitions grows, we will identify features concurrently with their assignment.

2. Molecular Orbital Calculations. The Fenske–Hall method has been used to investigate the bonding in $LMoOX_2$

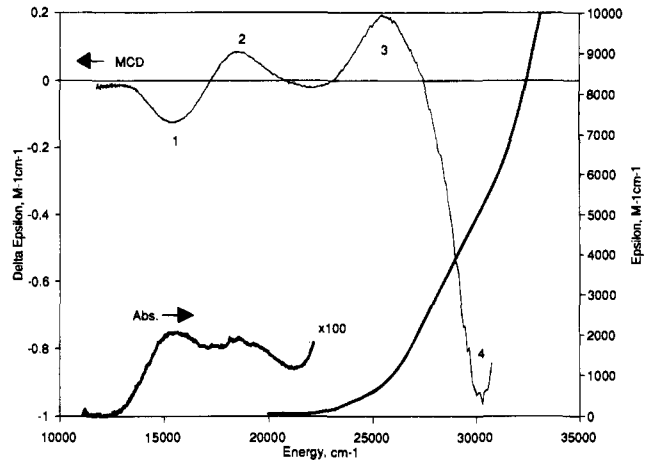

Figure 8. Room temperature absorption (bold line) and 5 K glass MCD (thin line) spectra of $LMoO(OCH_2CH_2O)$.

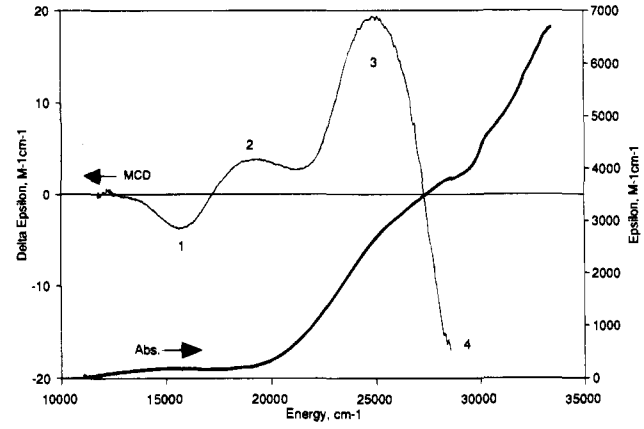

Figure 9. Room temperature absorption (bold line) and 5 K glass MCD (thin line) spectra of LMoO(catecholate).

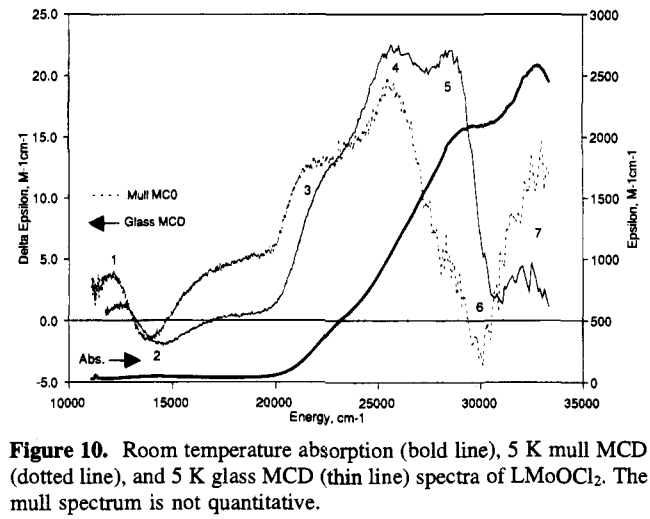

Figure 10. Room temperature absorption (bold line), 5 K mull MCD (dotted line), and 5 K glass MCD (thin line) spectra of $LMoOCl_2$. The mull spectrum is not quantitative.

(45) Reference 39, p 218.
(46) Kambli, U.; Gudel, H. *Inorg. Chem.* **1982**, *21*, 1270–1272.
(47) Reference 39, p 173.

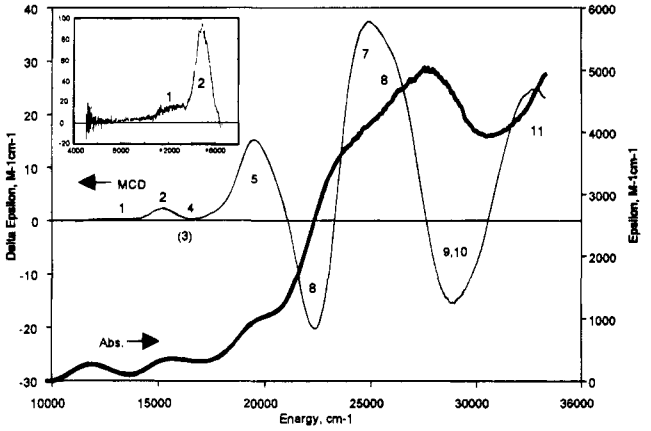

Figure 11. Room temperature absorption (bold line) and 5 K glass MCD (thin line) spectra of $LMoO(SCH_2CH_2S)$. Inset shows the near-IR MCD of a mulled sample at 5 K.

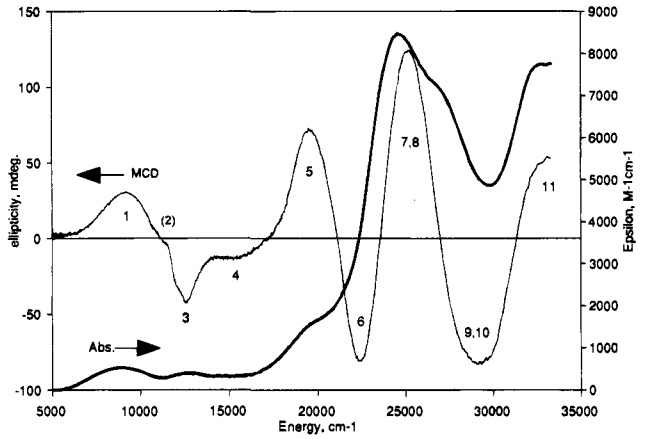

Figure 12. Room temperature absorption (bold line) and 5 K mull MCD (thin line) spectra of LMoO(toluene-3,4-dithiolate). The mull spectrum is not quantitative.

complexes and to provide a framework for interpreting the MCD spectra of the complexes. Figure 13 shows the coordinate system used for these calculations and the relative energies and primary character of the most important molecular orbitals. The standard group theoretical setting of axes for C_s places z normal to the $x-y$ mirror plane. In order to provide continuity with the C_{4v} compounds and continue using the standard C_{4v} notation for d orbitals, we have chosen a C_s coordinate system in which the z axis is parallel to the Mo=O bond and x and y point to the equatorial plane X groups. The HOMO is calculated in each case to be the singly occupied d_{xy} orbital which is consistent with experiment.[25] In Figure 13 all energies are relative to this HOMO, which is defined as zero. The C_s symmetry splits the degeneracy of the $d_{xz,yz}$ orbitals. The symmetry-adapted combinations of the $d_{xz,yz}$ orbitals in the coordinate frame of Figure 13 are referred to as $d_{x'z}$ (lying in the mirror plane) and $d_{y'z}$ (lying normal to the mirror plane). The ordering of the $d_{x'z}$ and $d_{y'z}$ orbitals will depend upon the relative interaction of these two orbitals (already split by the effects of the trispyrazolyl borate ligand) with the π-orbitals of the donor atoms, X. The $d_{x^2-y^2}$ and d_{z^2} orbitals occur at higher energy. Below the HOMO are the filled X ligand p lone pair orbitals. All of the $LMoOX_2$ complexes investigated possess donor atom π orbitals aligned perpendicular to the equatorial plane of the chelate (out-of-plane π orbitals). There is little change in the character of the out-of-plane π orbitals if the chelate ring is conjugated other than a further splitting of symmetric ($X\pi_s$) and antisymmetric ($X\pi_a$) orbitals in energy. For X = Cl, ligand in-plane π orbitals of a′

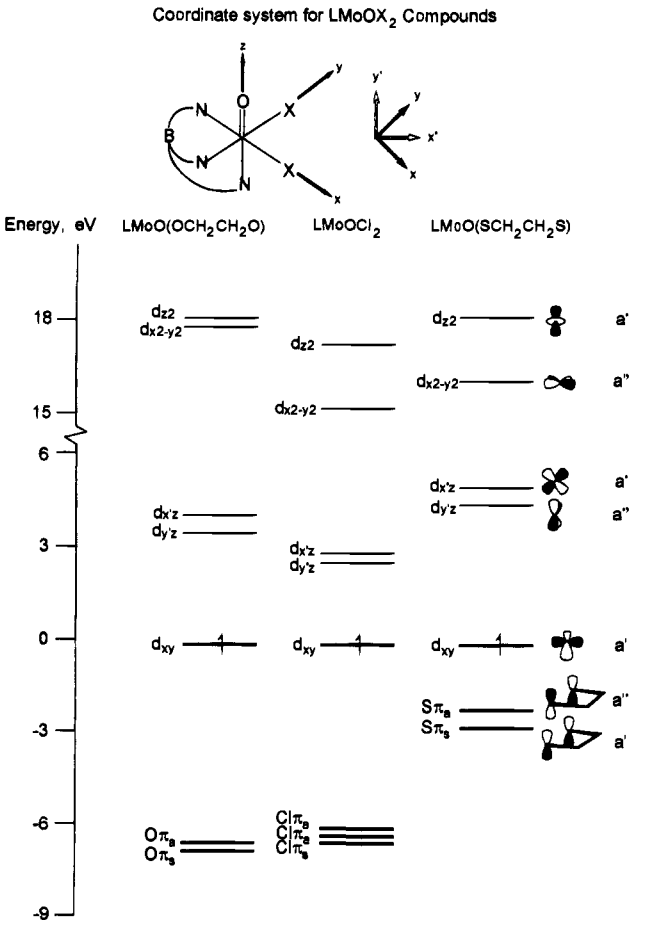

Figure 13. Partial molecular orbital energy level diagram of some $LMoOX_2$ complexes.

and a″ symmetry will also be present. The in-plane antisymmetric combination (a″) is the highest energy of the Clπ orbitals, followed by the π_a and π_s out-of-plane combinations. The symmetric in-plane Clπ orbital is stabilized by a small π-bonding interaction with d_{xy} and does not appear in Figure 13. When the X donor atoms are part of a chelate ring, then each donor atom will also have an "sp^2 hybrid" lone pair in the equatorial plane which also does not appear in Figure 13.

The general ordering of the d orbitals for the $LMoOX_2$ complexes of Figure 13 parallels that for C_{4v} symmetry (Figure 6), but the calculated energies of the virtual orbitals are substantially higher. It has been observed in other nonempirical Hartree-Fock calculations,[48] that the relative energies of excited states do not follow from the virtual orbitals considered in these types of calculations. We follow the calculated orderings, but spectroscopic determinations of the d−d transition energies in previously assigned molybdenyl compounds[49] provide a better estimate of the expected energy range of such transitions in these complexes. For the vast majority of molybdenyl complexes examined to date, ligand field transitions to the $d_{xz,yz}$ pair of orbitals have been observed within 12000−19000 cm^{-1} as a single broad band. Transitions to the $d_{x^2-y^2}$ orbital are observed in the 18000−28000 cm^{-1} region as a relatively narrow band whose energy is a measure of 10Dq for the equatorial ligands. No transitions to the d_{z^2} orbital have been unambiguously

(48) Garner, C. D.; Kendrick, J.; Lambert, P.; Mabbs, F. E.; Hillier, I. H. *Inorg. Chem.* **1976**, *15*, 1287−1291.

(49) Garner, C. D.; Charnock, J. M. In *Comprehensive Coordination Chemistry*; Wilkenson, G., Gillard, R. D., McCleverty, J. A., Eds.; Pergammon Press: New York, 1985; Vol. 3, pp 1329−1375 and references therein.

identified in molybdenyl compounds, and they are expected to lie at energies greater than 35000 cm^{-1} and be obscured by intense charge transfer transitions.[50] The energies of these charge transfer transitions will vary widely depending on the donor atom occupying the X positions. The orbitals commonly thought of as an sp^2 lone pair on thiols and alkoxides do not have substantial s character[51] but are still found to lie rather low in energy by our calculations; only in the case of sulfur might their charge transfer transitions be expected below 35000 cm^{-1}. The lowest energy charge transfer transitions are therefore expected to arise from the p-π type orbitals on the X ligands, which the molecular orbital calculations (Figure 6 and 13) place consistently as the SHOMO. In $[MoOCl_4]^-$, the first chlorine charge transfer transition occurs at 28000 cm^{-1} (Figure 7, band 4), Jørgenson's optical electronegativities[45] predict that alkoxide oxygen π charge transfer transitions will start at least 3000 cm^{-1} higher in energy than those originating from chlorine (>31000 cm^{-1}) and thiolate sulfur charge transfer transitions will begin at least 6000 cm^{-1} to lower energy (<22000 cm^{-1}). Thus, for oxygen donors the first three d−d transitions should occur below the X donor atom charge transfer, for chloride donors the third d−d transition may overlap the lowest energy charge transfer, and for sulfur donors, the d−d and lowest energy charge transfer transitions may be expected at similar energies.

VI. Analysis of $LMoOX_2$ Data

1. MCD Selection Rules. Selection rules for linearly polarized absorption in C_s symmetry predict that transitions will be polarized either normal to the mirror plane (y'), a′, or in the mirror plane (z or x'), a″, which leads through spin−orbit coupling, to (in first order) oppositely signed transitions in the MCD spectra[22,23] for each. Recognizing that the electronic structures of molybdenyl complexes are dominated by the $[Mo{=}O]^{3+}$ fragment and that this leads to close similarities in the overall bonding and ground states of pseudooctahedral molybdenyl compounds as the symmetry is lowered from C_{4v} to C_{2v} to C_s, it is reasonable to use the effective C_{4v} symmetry to predict the absolute signs of MCD transitions in lower symmetry complexes. We have already seen this holds for the quite small distortions of an axial ligand being added to $[MoOCl_4]^-$ (C_{4v} to C_{2v} [H_2O] or C_s[CH_3OH]).· Our Fenske−Hall calculations indicate that in the ground state, the metal d orbitals and the filled out-of-plane π-donor orbitals change little in energy or composition when the symmetry is lowered from idealized C_{4v} to C_{2v} and C_s. Experimentally, the EPR, absorption and MCD spectra[52] of $[MoO(SPh)_4]^-$, $[MoO(SCH_2CH_2S)_2]^-$, $LMoO(SCH_2CH_2S)$, and related compounds are found to be quite similar, suggesting that even this fairly drastic change in ligand set coupled with the symmetry reduction does not greatly perturb the ground state or basic bonding framework of molybdenyl complexes. We begin with the C_{4v} selection rules (Figure 7) and assume that an MCD transition between two specific molecular orbitals will maintain its sign under lower symmetry distortions. The $d_{x^2-y^2}$ orbital transforms as b_1 in C_{4v} and as a″ in C_s. The d_{xy} HOMO transforms as b_2 in C_{4v} and as a′ in C_s. The $d_{xy} \rightarrow d_{x^2-y^2}$ transition is easily identifiable based on absorption data alone and has a positive MCD transition for the C_{4v} compounds examined above. This transition specifies the sign of the transitions in C_s symmetry where all transitions fall into two classes. A positive MCD will be observed for transitions involving a change in symmetry (a″ ← a′), and a negative MCD will be observed for transitions between states of the same symmetry (a′ ← a′).

2. Band Assignments. Oxygen Donors: $LMoO(OCH_2CH_2O)$ and LMoO(catecholate). Figure 8 presents the absorption and MCD spectra of $LMoO(OCH_2CH_2O)$. The low-energy absorption band typical of molybdenyl compounds is split into two distinct peaks (bands 1 and 2) at 15600 and 19000 cm^{-1} (ϵ = 20 M^{-1} cm^{-1}). These peaks exhibit equal and opposite MCD intensity with the higher energy component being positive. The absorption and MCD spectra of LMoO(catecholate) (Figure 9) are strikingly similar to those for $LMoO(OCH_2CH_2O)$, but the differential and molar absorptivities for the band envelope near 15000 cm^{-1} for LMoO(catecholate) (ϵ = 190 M^{-1} cm^{-1}) is about 1 order of magnitude larger than that for $LMoO(OCH_2CH_2O)$. This low-energy peak is not split in the LMoO(catecholate) absorption spectrum, but exhibits a positive pseudo-A term in the MCD spectrum (bands 1 and 2). The small bite angle of the ethylene glycolate and catecholate ligands (approximately 80°)[53,11] places the chelate ring approximately in the equatorial plane and restricts the oxygen out-of-plane π-orbitals to be roughly parallel to the Mo=O bond. The negative feature in the MCD at 15000 cm^{-1} is assigned to the $a'(d_{xy}) \rightarrow a'(d_{x'z})$ transition; the positive feature at ca. 18500 cm^{-1} is assigned to the $a'(d_{xy}) \rightarrow a''(d_{y'z})$ transition. This energy ordering for the $d_{x'z}$ and $d_{y'z}$ orbitals is the opposite of that calculated in Figure 13 and that observed in $LMoOCl_2$ (Figure 10, *vide infra*).

The next feature, to higher energy, is a positive MCD peak (band 3) at 25200 cm^{-1} in $LMoO(OCH_2CH_2O)$ which is just inside the tail of rising absorbance intensity. The peak at 25000 cm^{-1} (band 3) of LMoO(catecholate) is substantially broader and more intense in both the MCD and absorption spectra than the corresponding peak in $LMoO(OCH_2CH_2O)$. These positive MCD features are reasonably assigned as the $a'(d_{xy}) \rightarrow a''(d_{x^2-y^2})$ transition.

A negative MCD feature (band 4) in $LMoO(OCH_2CH_2O)$ peaks at 30050 cm^{-1} corresponding to an intense absorption band (ϵ = 3940 M^{-1} cm^{-1}) at 28740 cm^{-1}. Our current data does not extend above 29000 cm^{-1} for LMoO(catecholate), but it is reasonable to associate a negative MCD peak (band 4) with the absorbance feature at 29410 cm^{-1}. A negative MCD feature near this energy is common to all the trispyrazolyl borate compounds and is probably due to a charge transfer transition involving the pyrazoyl ligands.

Halide Donor: $LMoOCl_2$. Figure 10 presents the absorption and MCD spectra for $LMoOCl_2$. The low-energy absorption band at 14180 cm^{-1} (ϵ = 50 M^{-1} cm^{-1}) gives rise to a pair of MCD peaks (bands 1 and 2) constituting a negative pseudo-*A* term. The weak absorption and pseudo-*A* behavior identify these as the $d_{xy} \rightarrow d_{x'z,y'z}$ transitions. The positive sign of the lower energy MCD component indicates that $d_{y'z}$ lies lower in energy than $d_{x'z}$. This energy ordering of the $d_{x'z,y'z}$ orbitals is found for other LMoOXY compounds in which X and Y are *monodentate* ligands,[54] but is opposite to that observed for the oxygen chelates above.

To higher energy, a positive MCD feature at 22000 cm^{-1} (band 3) corresponds to a shoulder in absorption at 22990 cm^{-1}. Band 3 is assigned to the $d_{x^2-y^2}$ transition due to its positive MCD and similar energy to that found in $[MoOCl_4]^-$. While the absorption intensity ($\epsilon \approx$ 500 M^{-1} cm^{-1}) is somewhat high

(50) Reference 39, p 395.
(51) Ashby, M. T. *Comments Inorg. Chem.* **1990**, *10*, 297−313.
(52) Goodwin, A. Ph.D. Dissertation, University of Manchester, England, 1989; pp 139−156.
(53) Chang, C. S. J. Ph.D. Dissertation, University of Arizona, Tucson, AZ, 1991.
(54) Carducci, M. D. Ph.D. Dissertation, University of Arizona, Tucson, AZ, 1994.

for a d−d transition, the same assignment has been proposed in other low-symmetry molybdenyl compounds.[55,25]

Further positive MCD features (bands 4 and 5) occur at ca. 26000 and 28000 cm^{-1}, the latter of which corresponds to an absorption peak at 29670 cm^{-1}. A weak negative MCD feature (band 6) is located at 30000 cm^{-1} and the absorption peak at 32500 cm^{-1} corresponds to a positive MCD peak (band 7). The remaining MCD features (bands 4−7) are assigned to charge transfer transitions. Band 4 is assigned to the a″ ← a′ transition from the antisymmetric in-plane chloride π orbitals to d_{xy}. The next positive feature (band 5) is assigned to the transition from the antisymmetric combination of the out-of-plane chloride π orbitals to d_{xy}. The symmetric combination of the out-of-plane chloride π orbitals should have a negatively signed component which we assign to band 6. However, as noted in the oxygen donors, this feature may instead or additionally be due to a transition involving the pyrazolyl ligands. The remaining positive feature (band 7) may be due to either an oxo or pyrazolyl charge transfer; both types of transitions are expected near this energy.

Sulfur Donors: LMoO(SCH_2CH_2S) and LMoO(toluene-3,4-dithiolate). The absorption and MCD spectra of LMoO(SCH_2CH_2S) and LMoO(toluene-3,4-dithiolate) are shown in Figures 11 and 12, respectively. In molybdenyl compounds containing multiple sulfur donors, it is difficult to uniquely identify d−d transitions since they are usually overlapped by more intense low-energy charge transfer transitions.[56−58] In addition to low-energy charge transfer transitions to the ground-state d_{xy} orbital, charge transfer transitions to the $d_{xz,yz}$ orbitals are also expected to occur within the energy range of this study. Their energies should be approximately the sum of the charge transfer to d_{xy} and the first ligand field transition (not taking into account differences in electron repulsion). In the Mo^{IV} compound[57] $[MoO(SC_6F_5)_4]^{2-}$, the lowest energy charge transfer transition is observed near 22200 cm^{-1} and has been assigned to $S\pi \rightarrow d_{xz,yz}$. Oxidation to Mo^{V} shifts this band to 18000 cm^{-1} and results in new weak charge transfer transitions at 7090 and 8580 cm^{-1}.[59] In $[Mo^{V}O(SCH_2CH_2S)_2]^{-}$, the corresponding weak low-energy feature was observed[52] near 10000 cm^{-1} by MCD, but not in the initial absorption spectra, indicating that care must be taken in examining the electronic spectra of molybdenyl compounds of thiolate ligands.

Figure 14 depicts a reasonable state diagram for LMoO(SCH_2CH_2S) and LMoO(toluene-3,4-dithiolate) along with the selection rules for transitions to each state. The proposed energy orderings have been derived from the spectra of Figures 11 and 12 and from the orbital orderings of the molecular orbital calculations (Figure 13), as described below. Only states expected to lie between 5000 and 35000 cm^{-1} are included in Figure 14.

Band 1, the lowest energy transition (12000 cm^{-1} in LMoO(SCH_2CH_2S), Figure 11, and 9000 cm^{-1} in LMoO(toluene-3,4-dithiolate), Figure 12) is assigned to the charge transfer transition from the a″ out-of-plane sulfur π_a orbital to d_{xy}. The positive MCD is as expected and the moderate absorption intensity is reasonable for a π out-of-plane to π in-plane charge transfer transition. Further, the energy in LMoO(toluene-3,4-dithiolate) is substantially lower than any reported

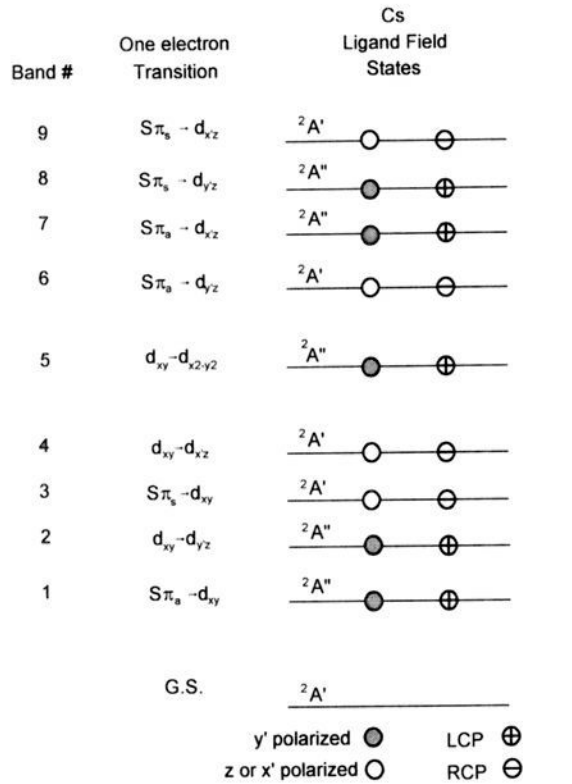

Figure 14. Proposed state diagram for LMoO(SCH_2CH_2S) and other compounds containing the $MoO(SR)_2$ fragment.

molybdenyl d−d transition and the shift to lower energy for the unsaturated ligand follows the trend expected from the MO calculations.

The remaining spectral features below 18000 cm^{-1} are more difficult to assign unambiguously. A negative feature arising from the a′ out-of-plane sulfur π_s orbital to d_{xy} and a negative/positive pair arising from the d_{xy} to $d_{x'z,y'z}$ transitions are all expected to occur in this region of the spectrum. For LMoO(SCH_2CH_2S) the weak symmetrical positive MCD feature at 15000 cm^{-1} can be assigned to $d_{xy} \rightarrow d_{y'z}$ (band 2 in Figures 11 and 14), and the return to zero can be assigned to $d_{xy} \rightarrow d_{x'z}$ (band 4 in Figures 11 and 14), which should have negative MCD. The negative counterpart of band 1 is not observed directly in the MCD spectrum. This expected negative MCD feature ($S\pi_s \rightarrow d_{xy}$, band 3 in Figure 14) should have weak intensity comparable to that of band 1 and is probably obscured by bands 2 and 5. For LMoO(toluene-3,4-dithiolate) only mull spectra could be obtained (Figure 12) and the MCD intensities are not quantitative. Nonetheless it is clear that the positive feature at 9000 cm^{-1} is followed by two negative MCD features between ca. 12000 and 16000 cm^{-1}. These negative features can be assigned to the $S\pi_s \rightarrow d_{xy}$ and $d_{xy} \rightarrow d_{x'z}$ transitions (bands 3 and 4 of Figure 14), but their relative order cannot be specified. Figure 14 predicts a fourth feature (band 2) in this energy region which would be positive in sign and is the counterpart of band 4. We suggest that two overlapping positive MCD transitions make up the feature labeled band 1 in Figure 12.

The above interpretation of the low-energy (<18000 cm^{-1}) MCD features of LMoO(SCH_2CH_2S) and LMoO(toluene-3,4-dithiolate) is consistent with positive−positive−negative−negative MCD features for both compounds, but only three of these features can be clearly identified in each case. Our proposed assignments of the relative ordering of bands 1 and 2 and of bands 3 and 4 cannot be unambiguously specified from the available data. Moreover, second-order spin−orbit coupling

(55) Pence, H. E.; Selbin, J. *Inorg. Chem.* **1969**, *8*, 353−358.
(56) Hanson, G. R.; Brunette, A. A.; McDonell, A. C.; Murray, K. S.; Wedd, A. G. *J. Am. Chem. Soc.* **1981**, *103*, 1953−1959.
(57) Ellis, S. R.; Collison, D.; Garner, C. D. *J. Chem. Soc., Dalton Trans.* **1989**, 413−417.
(58) Ueyama, N.; Okamura, T.; Nakamura, A. *J. Am. Chem. Soc.* **1992**, *114*, 8129−8137.
(59) Preliminary spectroelectrochemical measurements on $LMo^{(V,IV)}O(SR)_2$ compounds produce similar changes in absorbance.[62]

of the charge transfer and ligand field states, as is observed in $[MoOCl_4]^-$ (*vide supra*), would further complicate making unambiguous assignments.

From 18000 to 35000 cm^{-1} the MCD and absorption spectra of $LMoO(SCH_2CH_2S)$ and LMoO(toluene-3,4-dithiolate) are almost identical. Both have a positive MCD peak (band 5) which corresponds with the absorption peak at 20000 cm^{-1}. Peak maxima in the absorption spectra at 23500 and 28200 cm^{-1} and 24900 and 27400 cm^{-1}, respectively, correspond to crossing points in the MCD spectrum suggesting two overlapping pseudo-*A* terms, the first positive (bands 6 and 7) and the second negative (bands 8 and 9) with their positive components overlapping. Neither of the remaining MCD features have corresponding features in the absorption spectra; a negative MCD peak (band 10) would account for the breadth of the MCD troughs at 29300 and 30000 cm^{-1}, while a positive feature (band 11) peaks at 33000 and 34000 cm^{-1}.

The positive MCD peak at 20000 cm^{-1} is assigned to the d_{xy} to $d_{x^2-y^2}$ transition (band 5). The low energy of this transition compared with the previous compounds is consistent with thiolate being the weakest field ligand of those that have been examined. As with $LMoOCl_2$ (Figure 10), the absorption intensity is large for a d−d transition, but not unreasonable considering the low symmetry and substantial S ligand p contribution (20% in our MO calculations) to this Mo−S σ^* orbital. The negative−positive−positive−negative C-term pattern from 21000 to 29000 cm^{-1} corresponds to two peaks in the absorption spectra. This pattern is precisely what is expected for the charge transfer transitions from the two out-of-plane sulfur π orbitals to the $d_{y'z}$ and $d_{x'z}$ orbitals, as depicted in Figure 14 (bands 6−9). The high absorption intensity is as expected for a π out-of-plane to π out-of-plane transition compared to the π out-of-plane to π in-plane transition that occurs to the d_{xy} orbital (bands 1 and 3). This pattern fixes the order of the $d_{y'z}$ and $d_{x'z}$ orbitals to be the same as that observed for the monodentate compounds and opposite to that found for the oxygen chelates, indicating that the bond angle between X ligands is not solely responsible for determining their energy ordering.

The final features, bands 10 and 11, analogous to $LMoOCl_2$, are tentatively assigned to charge transfer involving pyrazolyl ligands; however, further sulfur based charge transfer transitions are also expected to be in this energy region.

VII. Comparison of MCD Data from DMSO Reductase with Models

The MCD spectra of native[23] and glycerol inhibited[24] DMSO reductase are similar to each other in appearance, but the corresponding bands for the *native* form are shifted to higher energy by approximately 900 cm^{-1} and exhibit differential absorbencies that are only about one-fourth as intense as those of the inhibited form. In Figure 15 the MCD spectrum of the *glycerol-inhibited* Mo(V) form of DMSO reductase[24] is replotted as a function of energy and overlaid on our MCD spectrum of $LMoO(SCH_2CH_2S)$ in the same energy region. The low-energy region of this enzyme spectrum was not included in the published figure, but a broad weak negative MCD band at ≈11000 cm^{-1} has been described.[24] Considering the differences in temperature and magnetic field strength of the data collections, the *native* form and our model show comparable differential absorbance values between 20000 and 30000 cm^{-1}, as do other sulfur containing model compounds.[52] Comparison of the two spectra show some general similarities and some marked differences. Both spectra show a medium intensity positive peak near 20000 cm^{-1} and weak absorbance near 11000 cm^{-1}. From 21000 to 30000 cm^{-1} the enzyme and model exhibit peaks at similar energies and intensites, but of *opposite* sign. The striking difference between the two spectra is the intense positive pseudo-*A* term in the enzyme spectra at 15000 cm^{-1} which is not present in the spectra of our thiolate containing model compounds.

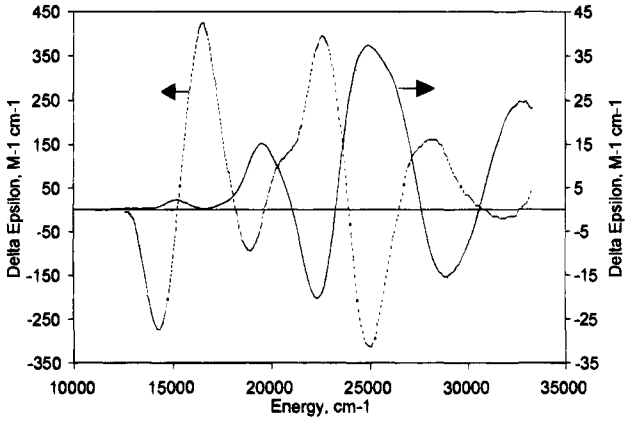

Figure 15. Comparison of the MCD spectrum from the glycerol inhibited Mo(V) form of DMSO reductase[24] (dotted line) at 4.5 T and 1.6 K with the MCD spectrum of $LMoO(SCH_2CH_2S)$ (thin line) at 5.0 T and 4.2 K. Note the different scales and conditions for the two spectra.

Both reports of the MCD spectra of DMSO reductase have analyzed the observed spectrum in terms of charge transfer transitions in a simple C_{2v} model that consists of Mo(V) ligated by a single dithiolene ligand, but neither analysis included the effects of the terminal oxo group of the molybdenyl fragment that is known to be present in the enzyme. The MCD bands have been assigned[23,24] to charge transfer transitions from three filled dithiolene π orbitals to the two lowest lying metal d orbitals. We propose a modified interpretation of the MCD spectra of DMSO reductase based upon our investigations of the MCD spectra of model oxo-Mo(V) complexes presented above (Figures 11−14). Our interpretation rests on two key observations. (1) The terminal oxo group dominates the splitting of the metal d orbitals in both high- and low-symmetry complexes for all types of donor atoms.[60] (2) The filled π orbital of dithiolene ligands that is primarily the C=C π bond is substantially lower in energy than the sulfur π orbitals of the ligand. PES spectroscopy places this orbital 16000 cm^{-1} lower in energy for thiomethyl-substituted ethylenes,[61] and molecular orbital calculations on molybdenyl−monodithiolene fragments suggest that such a transition would be much higher in energy than Sπ to metal $d_{xz,yz}$ charge transfer transitions.[62] There is no experimental evidence for a charge transfer transition from this filled π orbital to Mo in the MCD spectra of model complexes because $LMoO(SCH_2CH_2S)$ (saturated ligand skeleton) and LMoO(toluene-3,4-dithiolate) (unsaturated ligand skeleton) show very similar spectral features. This orbital is not included in the energy diagram for sulfur donors in Figure 13 and is not expected to contribute to the spectrum of the enzyme.

The dominance of the oxo group in determining the d orbital splittings of the Mo atom and the low energy of the C=C π bond in monodithiolenes, suggest that the state diagram developed here for $LMoOX_2$ compounds (Figure 14) may also be used to interpret the MCD spectra of DMSO reductase. We

(60) Nugent, W. A.; Mayer, J. M. *Metal-Ligand Multiple Bonds*; Wiley-Interscience: New York, 1988.
(61) Gleiter, R.; Spanget-Larsen, J. *Top. Curr. Chem.: Spectrosc.* **1979**, *86*, 139−196.
(62) Carducci, M. D.; Enemark, J. H. Unpublished results.

consider three possible explanations for the differences observed between the MCD spectra of DMSO reductase and the model compounds containing chelating thiolate ligands (Figure 15). (1) The active site of DMSO reductase is structurally similar to our model compounds, but the other ligating atoms at the metal site lead to an inversion of the energies of the $d_{x'z}$ and $d_{y'z}$ orbitals compared to the model compounds. This study has shown that the relative energies of the $d_{x'z}$ and $d_{y'z}$ orbitals depend on the ligands in the equatorial plane of the complex. In terms of the state diagram (Figure 14), this would switch not only bands 2 and 4, but bands 6 and 7 and bands 8 and 9 as well, resulting in an expected positive−negative−negative−positive feature and effecting a change of sign for the transitions between 21000 and 30000 cm^{-1}. The positive peak near 20000 cm^{-1} would be the ligand field $d_{xy} \rightarrow d_{x^2-y^2}$ transition. The weak band at $\approx$11000 cm^{-1} is lower in energy than any reported molybdenyl ligand field band[53,63] and is probably a weak sulfur to molybdenum charge transfer transition. (2) The active site of DMSO reductase possesses additional sulfur atoms (EXAFS studies of related oxomolybdenum enzymes indicate up to four coordinated sulfur atoms).[2] Additional sulfur atoms could give rise to the intense pseudo-*A* term at $\approx$15000 cm^{-1}, while maintaining the pattern expected for two sulfur atoms in the equatorial plane. (3) Available structural data for oxo-Mo(IV/V) model compounds[49] suggest that sulfur atoms prefer to coordinate cis to the single terminal oxo group. However, an alternative geometry may exist at the active site of DMSO reductase that is not related to the pseudooctahedral complexes with two sulfur donors in the equatorial plane examined here. In the absence of MCD data from well-defined compounds with alternative coordination numbers, geometries, and stereochemistries, it is not possible to eliminate explanation 3 at this point.

VIII. Discussion

MCD studies on a series of oxo-Mo(V) complexes of known stereochemistry have enabled the MCD spectra of low symmetry (C_s) complexes to be assigned by relating the observed spectra to those from higher symmetry (C_{4v}) species. For $LMoOX_2$ complexes with sulfur donor atoms, overlap of the low-energy charge transfer bands and the lowest energy d−d bands makes it difficult to unambiguously assign the spectra below 15000 cm^{-1}. We have assigned the lowest energy absorption band to a charge transfer transition from an out-of-plane $S\pi$ orbital to Mo d_{xy}. This presence of a low-energy charge transfer transition supports the idea that the large g values ($g_1 > 2.00$) observed in such compounds result from positive contributions to g from charge transfer terms that are comparable to or even outweigh the contributions from d $\rightarrow$ d terms, which act to lower the g value.[25,64] The transition from the HOMO (d_{xy}) to $d_{x^2-y^2}$ and the charge transfer transitions from the filled $S\pi$ orbitals to $d_{x'z,y'z}$ can be assigned with more confidence. The MCD spectra of the sulfur containing model complexes strongly suggest that $S\pi$ to Mo(d_{xy}) and $S\pi$ to Mo($d_{xz,yz}$) charge transfer transitions are the dominant features in the MCD spectra of molybdenyl centers with the stereochemistry found in Figure 1. The differences in the MCD spectral patterns between the models and DMSO reductase may reflect a different coordination geometry and/or additional sulfur ligands for the enzyme.

The MCD spectra of the model compounds analyzed here should provide a basis for interpreting the MCD data from other oxo-Mo(V) compounds especially those with sulfur donor ligands. However, additional MCD data on oxo-Mo(V) complexes with alternative stereochemical relationships between the terminal oxo group and the sulfur donor ligands are needed in order to more definitively relate the MCD spectra of DMSO reductase and other Mo enzymes to specific stereochemistries.

Finally, these spectral studies of molybdenyl complexes provide significant insight into the electronic structure contributions to catalysis by oxomolybdenum enzymes. The proposed catalytic cycles for these enzymes involve both atom transfer and electron transfer reactions.[1,2] Substrate oxidation (reduction) is proposed to involve oxygen atom transfer between the substrate and the $Mo^{IV}O$ and $Mo^{VI}O_2$ forms of the molybdenum center.[1,2,65] Holm[65] has suggested that the role of sulfur coordination to molybdenum is to destabilize the oxidized $Mo^{VI}O_2$ state in order to facilitate cleavage of the Mo=O bond during the catalytic cycle. The energies and intensities of the MCD bands for well-characterized $LMo^{V}OX_2$ complexes with chelating sulfur ligands indicate that the filled sulfur π orbitals are close in energy to and can strongly covalently overlap with the molybdenum d orbitals; π donation from these filled sulfur orbitals will compete with π donation from the terminal oxo group to weaken the Mo=O bond. The observed Mo=O stretching frequencies for analogous $LMo^{V}OX_2$ complexes are 10−15 cm^{-1} lower for X = S compared to X = O, reflecting this effect.[25,66]

Regeneration of the catalytic molybdenum center following oxygen atom transfer to the substrate is proposed to involve two successive one-electron transfers, passing through the $Mo^{V}O$ state.[1,2] The low-energy sulfur to molybdenum charge transfer bands of moderate intensity observed for $LMo^{V}O(SCH_2CH_2S)$ and $LMo^{V}O$(toluene-3,4-dithiolate) in this work show that the filled sulfur π orbitals are close in energy to and overlap significantly with the d_{xy} orbital whose occupancy changes during the one-electron steps. These sulfur orbitals should provide an effective low-energy super exchange pathway for the one-electron transfers that interconvert the Mo(IV,V,VI) states during the catalytic cycle. Recent studies show that for $LMo^{V}OX_2$ complexes with chelating X_2 ligands the rates of heterogeneous electron transfer for the Mo(V/IV) couple with X = S are about 1.5 orders of magnitude faster than those for analogous compounds with X = O.[67] Thus, sulfur ligation of oxomolybdenum centers leads to electronic structures that facilitate both the oxygen atom and electron transfer reactions that are proposed to occur in the catalytic cycles of these enzymes.

Acknowledgment. We gratefully acknowledge Dr. Jesse Chang and Dr. Michael LaBarre for their synthetic contributions to this project. Dr. Paul Ross, Dr. Michael Baldwin, Joe Foroughi, Dr. Cecelia Campochiaro, and Dr. Marty Kirk are thanked for many helpful discussions and experimental assistance. We thank Dr. Nikolai Shokhirev for assistance in performing spin−orbit coupling calculations. For insightful discussions and a copy of ref 52 we thank Dr. David Collison. We thank Dr. A. Gewirth for a preprint of ref 34 and Dr. F. A. Schultz for a preprint of ref 67. Financial support from the National Institutes of Health (Grant No. GM-37773 to J.H.E.) and the National Science Foundation (Grant No. CHE-9217628 to E.I.S.) is gratefully acknowledged.

(63) Reference 39, p 394.
(64) Mabbs, F. E.; Collison, D. *Electron Paramagnetic Resonance of d Transition Metal Compounds*; Elsevier Science Publishers B.V.: Amsterdam, The Netherlands, 1992.
(65) Holm, R. H. *Coord. Chem. Rev.* **1990**, *100*, 183−221.
(66) Chang, C. S. J.; Collison, D.; Mabbs, F. E.; Enemark, J. H. *Inorg. Chem.* **1991**, *29*, 2261−2267.
(67) Olson, G. M.; Schultz, F. A. *Inorg. Chim. Acta* **1994**, in press.